

## Microcontact Printing



## Writing Patterns of Molecules on Molecular Printboards\*\*

Tommaso Auletta, Barbara Dordi, Alart Mulder, Andrea Sartori, Steffen Onclin, Christiaan M. Bruinink, Mária Péter, Christian A. Nijhuis, Hans Beijleveld, Holger Schönherr, G. Julius Vancso, Alessandro Casnati, Rocco Ungaro, Bart Jan Ravoo, Jurriaan Huskens,\* and David N. Reinhoudt\*

Bottom-up nanotechnology has to start with the precise positioning of molecules. For this purpose we are developing molecular printboards, that is, self-assembled monolayers (SAMs) of molecules that have specific recognition sites, for example, molecular cavities, to which molecules can be anchored through specific and directional supramolecular interactions.<sup>[1]</sup> Such molecular printboards are prepared by the self-assembly of  $\beta$ -cyclodextrin ( $\beta$ -CD) derivatives on

gold and silicon oxide surfaces. Herein we describe how to print or write, by microcontact printing ( $\mu$ CP) and dip-pen nanolithography (DPN), respectively, molecular patterns of guest-functionalized calixarene molecules, dendritic wedges labeled by fluorescent groups, and dendrimers on  $\beta$ -CD-terminated printboards. The binding, as well as the desorption of the molecules, can be fine-tuned by chemical design, which allows virtually unlimited flexibility in the chemical functions that can be employed. These structures can be subsequently used to direct the adsorption of different materials, for example, fluorescent dyes.

Microcontact printing has been developed by Whitesides for the preparation of patterns of molecules on bare surfaces by, for example, the transfer of thiols to gold substrates in the contact areas between a soft polymeric stamp and the substrate.<sup>[2,3]</sup> This has recently been extended by Mirkin and co-workers to writing with molecules on such surfaces by using the DPN approach.<sup>[4]</sup> Various types of molecules were deposited onto different substrates by DPN which led to arrays of, for example, DNA,<sup>[5]</sup> proteins,<sup>[6]</sup> and nanoparticles.<sup>[7]</sup> Registry capabilities have been demonstrated as well,<sup>[8]</sup> and a multipen nanoplotter able to produce parallel patterns with different ink molecules has been developed.<sup>[9]</sup>

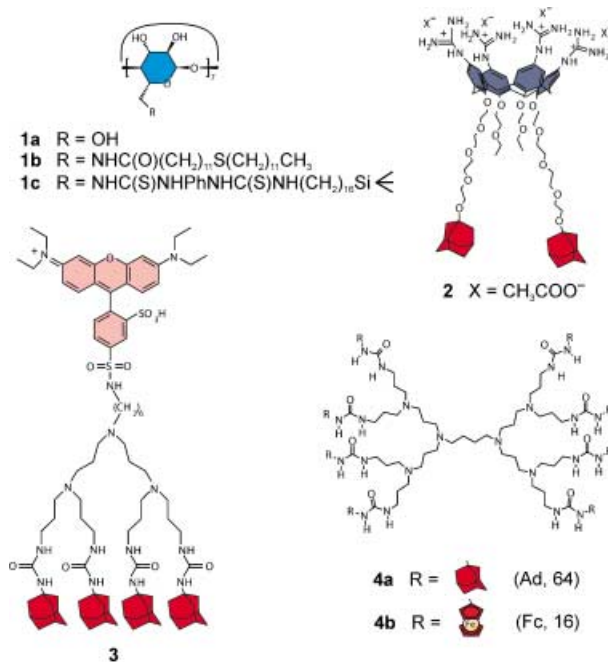
$\beta$ -CD (**1a**, Scheme 1) can act as a host for the binding of a variety of small, organic guest functionalities in water through hydrophobic interactions. We prepared self-assembled monolayers (SAMs) of a  $\beta$ -CD heptathioether adsorbate **1b** (Scheme 1) on gold as described before.<sup>[10,11]</sup> Such adsorbates form densely packed, well-ordered SAMs with equivalent

[\*] Dr. T. Auletta, A. Mulder, S. Onclin, C. M. Bruinink, Dr. M. Péter, C. A. Nijhuis, H. Beijleveld, Dr. B. J. Ravoo, Dr. J. Huskens, Prof. Dr. D. N. Reinhoudt  
University of Twente, MESA<sup>+</sup> Institute for Nanotechnology Supramolecular Chemistry and Technology  
P.O. Box 217, 7500 AE Enschede (The Netherlands)  
Fax: (+31) 53-4894645  
E-mail: j.huskens@utwente.nl  
d.n.reinhoudt@utwente.nl

B. Dordi, Dr. H. Schönherr, Prof. Dr. G. J. Vancso  
University of Twente, MESA<sup>+</sup> Institute for Nanotechnology Materials Science and Technology of Polymers  
P.O. Box 217, 7500 AE Enschede (The Netherlands)  
A. Sartori, Dr. A. Casnati, Prof. Dr. R. Ungaro  
Università degli Studi di Parma  
Dipartimento di Chimica Organica e Industriale  
Parco Area delle Scienze 17A, 43100 Parma (Italy).

[\*\*] The support given by the Netherlands Organization for Scientific Research (NWO; grant 97041), the Applied Science division of the NWO and the Ministry of Economic Affairs (STW; TST 4946), and the MESA<sup>+</sup> Institute for Nanotechnology is gratefully acknowledged. Tascon GmbH (Münster, Germany) is gratefully acknowledged for the SIMS measurements.

Supporting information for this article is available on the WWW under <http://www.angewandte.org> or from the author.



**Scheme 1.** Structures of  $\beta$ -cyclodextrin ( $\beta$ -CD, **1a**) and  $\beta$ -CD adsorbates **1b** and **1c** for attachment to gold and silicon oxide, respectively; bis(adamantyl)-functionalized calixarene (**2**); lissamine-rhodamine B functionalized dendritic wedge (**3**); generic second generation PPI dendrimer with 8 R groups: **4a** has 64 Ad moieties (fifth generation) and **4b** has 16 Fc moieties (third generation).

binding sites, the near-hexagonal packing of which can be visualized by AFM.<sup>[11]</sup>

We have measured the interaction thermodynamics of these  $\beta$ -CD-terminated printboards with several guests, by using a variety of techniques, including AFM dynamic force spectroscopy, which allows the detection of individual rupture forces of host–guest complexes.<sup>[12]</sup> The binding of small, univalent guest molecules to these SAMs has been studied by surface plasmon resonance (SPR)<sup>[13]</sup> and electrochemical impedance spectroscopies (EIS).<sup>[11]</sup> An important finding from these studies was that the interaction strength of such guest molecules with  $\beta$ -CDs on the printboards is identical to the binding strength in solution.<sup>[13]</sup> The binding of large dendrimers functionalized with adamantyl (Ad) groups through multiple interactions has also been recently discussed.<sup>[1]</sup>

Multivalency, that is, the use of multiple interactions which are assumed to act in a stepwise, independent assembly process, is of strong current interest<sup>[14]</sup> for its implications in the design of new ligands and inhibitors for proteins because it offers a tool for fine-tuning overall interaction strengths. It has been, for example, employed in the development of high-affinity vancomycin–peptide systems,<sup>[15]</sup> which has very recently been extended to the assembly of vancomycin-functionalized polymers at peptide SAMs.<sup>[16]</sup> Therefore, the use of molecules which allow the formation of *multiple* supramolecular interactions constitutes a tool to tune adsorption and desorption process parameters at surfaces—thermodynamics and kinetics are in principle related in a straightforward manner to the number of interactions and to the strength and kinetics<sup>[17]</sup> of an individual interaction. Thus, we synthesized the water-soluble calix[4]arene **2** which contains two Ad moieties as the guest motif (Scheme 1). The binding of **2** with  $\beta$ -CD in solution and onto  $\beta$ -CD-terminated SAMs was investigated by microcalorimetry and SPR, respectively. The binding behavior with  $\beta$ -CD in water showed the two Ad groups bound independently<sup>[18]</sup> to two separate  $\beta$ -CDs, with binding parameters characteristic of Ad– $\beta$ -CD interactions.<sup>[13]</sup> The binding constant  $K$  obtained for this guest with a  $\beta$ -CD dimer<sup>[19]</sup> was  $1.4 \times 10^7 \text{ M}^{-1}$ , based on a 1:1 model.<sup>[20]</sup> The interaction with the  $\beta$ -CD-terminated SAMs appeared to be much stronger ( $K = 10^9$ – $10^{10} \text{ M}^{-1}$ ),<sup>[21]</sup> which is ascribed to the high local concentration of hosts at the surface.<sup>[1]</sup>

Such interaction strengths are already sufficiently high to apply these molecules in nanofabrication as, for example, in  $\mu$ CP. We employed, for the first time, *supramolecular*  $\mu$ CP, which is the transfer of molecules from a stamp to a surface to give specific host–guest assemblies on the printboards. Patterns were visible directly after printing and remained clearly visible when rinsed with substantial amounts of water or 50 mM aqueous NaCl (Figure 1).<sup>[22]</sup> Even prolonged washing with  $\beta$ -CD in solution, to promote competition between the host–guest binding in solution and at the printboard, did not completely remove the patterns. The presence of the guest molecules in the contacted areas was also confirmed by secondary ion mass spectrometry (SIMS) imaging, as shown

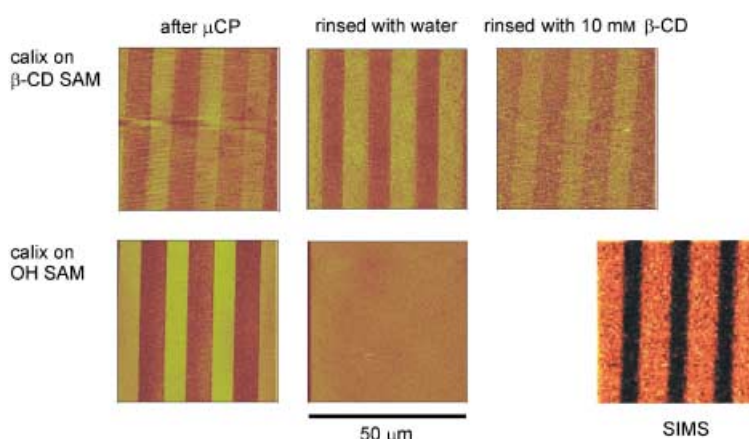


**Figure 1.** AFM friction force images (acquired in air) of patterns obtained by  $\mu$ CP of the calixarene guest **2** (brighter areas) on  $\beta$ -CD- (top) and OH-terminated SAMs (bottom): before rinsing, after rinsing with Milli-Q water, or after rinsing with 10 mM aqueous  $\beta$ -CD, respectively (image size  $50 \times 50 \mu\text{m}^2$ ; friction forces (a.u.) increase from dark to bright contrast). SIMS-TOF image of a  $\beta$ -CD-terminated SAM after printing of **2** (image size:  $56 \times 56 \mu\text{m}$ ): the bright areas indicate the presence of the molecular ion peak at  $m/z = 1418$ .

for an image of the molecular ion peak of the calixarene **2** (Figure 1).

The requirement of specific host–guest interactions for sustained pattern stability is evident when  $\mu$ CP on the  $\beta$ -CD-terminated SAMs is compared to  $\mu$ CP on 11-sulfanyl-1-undecanol SAMs (OH SAMs) on gold (Figure 1). Ink transfer also occurs on the OH SAMs, but patterns were instantly removed upon washing with water or 50 mM aqueous NaCl.

We also employed supramolecular DPN to write local patterns of molecules on the printboard (Figure 2). Silicon nitride AFM tips were dipped into an aqueous solution of the calixarene (**2**) ink and scanned across  $\beta$ -CD- as well as OH-modified SAMs. The transfer of ink was observed for both SAMs, but patterns stable to rinsing were only obtained for the  $\beta$ -CD printboards (Figure 2, left). As a control experiment, a  $\beta$ -CD-terminated SAM was scanned with a bare  $\text{Si}_3\text{N}_4$  tip under the same experimental conditions reported above for the writing experiment. Subsequent AFM friction force imaging did not show any visible pattern on the surface. This result proves that the structures of Figure 2 do not arise from mechanical forces applied by the tip to the SAM, but rather by the transfer of ink molecules. The resolution that can be attained by this technique is well below 100 nm, as shown by the line patterns in Figure 2 (right). It is likely to be a function of contact time, tip radius, ink concentration, and ink-transfer mechanism, as in traditional DPN.

To widen the scope of the supramolecular patterning approaches described above, we also prepared  $\beta$ -CD printboards on silicon oxide (**1c**, see Supporting Information) because  $\text{SiO}_2$  permits fluorescence detection of the assemblies, whereas quenching occurs for SAMs on gold. Micro-contact printing of the calixarene guest **2** gave results similar to the  $\beta$ -CD-terminated SAMs on gold, both in regard to ink transfer and pattern stability. The printing of fluorescent dendritic wedge **3** (Scheme 1), which was transferred as the per- $\beta$ -CD complex, allowed pattern detection by confocal

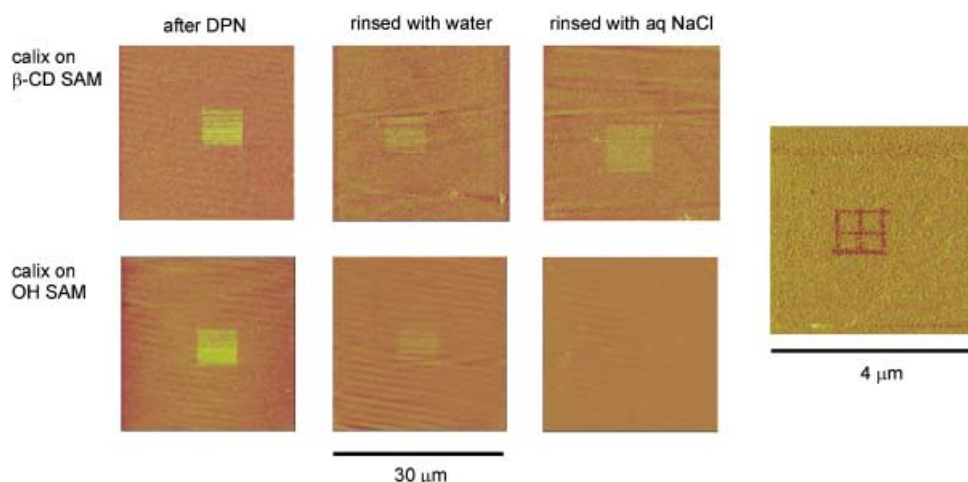


**Figure 2.** Left: AFM friction force images (friction forces (a.u.) increase from dark to bright contrast) showing, from left to right, patterns produced by DPN on a  $\beta$ -CD-terminated SAM (top) and on an OH-terminated SAM (bottom) using **2** as the ink before rinsing (image acquired in water), after rinsing in situ with Milli-Q water (image acquired in water), and with 50 mM aqueous NaCl (image acquired in aqueous NaCl), respectively. Right: AFM friction force images in air of arrays of lines with mean widths ( $\pm$  standard deviation) of  $60 \pm 20$  nm produced by DPN (friction inversion with respect to the  $\mu$ CP experiments is related to the AFM tip employed in the imaging step, which is the same as in the writing step and thus still covered with the molecular ink). For DPN, cleaned  $\text{Si}_3\text{N}_4$  tips were coated with the calixarene ink by soaking them for 15 min in a 0.5 mM aqueous solution of **2** and drying, and then scanned twice across a  $7 \times 7 \mu\text{m}^2$  area of a SAM on gold (scan velocity ca.  $21 \mu\text{m s}^{-1}$ ,  $T = 25^\circ\text{C}$ , relative humidity  $47 \pm 3\%$ ). The scan size was then increased to  $30 \times 30 \mu\text{m}^2$ , the scan velocity was set to  $100\text{--}300 \mu\text{m s}^{-1}$  and the relative scan angle was adjusted accordingly. The lines were produced by scanning each line for a 40 s period (scan velocity was ca.  $2 \mu\text{m s}^{-1}$ ,  $T = 25^\circ\text{C}$  and relative humidity  $47 \pm 3\%$ ). The scan size was then increased to  $4 \times 4 \mu\text{m}^2$ , and the scan velocity increased to  $30 \mu\text{m s}^{-1}$ . The tip was withdrawn prior to rinsing. The AFM liquid cell was then flushed with 5 mL of Milli-Q water and new images were recorded. Eventually the cell was flushed with 5 mL of 50 mM aqueous NaCl, before new images were recorded.

microscopy (Figure 3, top). Rinsing the surface with a 10 mM aqueous phosphate buffer hardly affected the printed patterns, as witnessed in this case by monitoring fluorescence intensities. Only rinsing with 10 mM  $\beta$ -CD led to a significant reduction of the fluorescence.<sup>[23]</sup>

Patterns of a fifth generation Ad-terminated poly(propylene imine) dendrimer **4a** (Scheme 1), functionalized with 64 Ad end groups,<sup>[24]</sup> on  $\beta$ -CD printboards on silicon oxide were created by supramolecular  $\mu$ CP. Such molecules behave as molecular boxes for dyes through electrostatic interactions, both as the free box<sup>[25]</sup> and as complexes with  $\beta$ -CD in aqueous solution.<sup>[24]</sup> The dendrimers were printed as the per- $\beta$ -CD complex. The dendritic boxes were subsequently loaded with two different fluorescent dyes (either fluorescein or rose bengal) by immersing the patterned substrates into aqueous solutions of these dyes (Figure 3, bottom).

We can also use electroactive third generation dendrimers **4b** terminated with ferrocene (Fc; Scheme 1) as the ink (as they also form inclusion complexes with  $\beta$ -CD<sup>[26]</sup>) to control the desorption of the host–guest assemblies electrochemically. The Fc-functionalized dendrimers were adsorbed from solution onto the  $\beta$ -CD printboards on gold. The known oxidation of the Fc groups to ferrocenium cations that leads to complete loss of the Fc– $\beta$ -CD interaction<sup>[26]</sup> provides us with a tool to induce desorption by an external (electrochemical) stimulus in an electrochemical setup where the gold

layer of the  $\beta$ -CD printboard acts as the working electrode. Sequential cyclic voltammograms of a monolayer of Fc-modified dendrimer **4b** on the  $\beta$ -CD printboard showed a decrease in the peak current that corresponds to a decrease in the amount of adsorbed material (see the Supporting Information). Peak currents remained constant when the cyclic voltammograms were recorded in the presence of the dendrimer **4b** in solution, which indicates that oxidized and desorbed dendrimers were constantly being replaced by nonoxidized molecules from solution.

In summary, we have shown that molecular printboards allow for versatile nanofabrication schemes of printing and writing that are applicable to various types of substrates and molecules. Their advantages lie in the tunability of the type and number of host–guest motifs and the possibility to erase patterns. Only a limited number of such supramolec-

ular interactions per guest molecule are required for the formation of stable patterns, thus eliminating the need for very complicated synthesis. Molecular printboards will open up ways to fabricate arrays of multiple host–guest systems, to study the formation and dynamics of individual supramolecular assemblies at surfaces, and for the preparation of 3D supramolecular architectures on substrates.

### Experimental Section

The synthesis of the  $\beta$ -CD adsorbate **1b** and the preparation of SAMs on Au substrates were reported previously.<sup>[10,11]</sup> The synthesis of adsorbate **2**, of lissamine–rhodamine B/poly(propylene imine) dendritic wedge **3**, and the preparation of monolayers on silicon oxide are reported in the Supporting Information. The fifth generation adamantane-terminated poly(propylene imine) dendrimer (G5-PPI-(Ad)<sub>64</sub>) **4a**, the third generation ferrocene-terminated poly(propylene imine) dendrimer (G3-PPI-(Fc)<sub>16</sub>) **4b**, and their per- $\beta$ -CD complexes were synthesised according to literature procedures.<sup>[24,27]</sup> Microcontact printed substrates were prepared according to literature procedures.<sup>[2]</sup>

Calorimetric titrations were performed at  $25^\circ\text{C}$  using a Microcal VP-ITC isothermal titration microcalorimeter. Titrations of **2** with native  $\beta$ -CD or a  $\beta$ -CD dimer<sup>[19]</sup> were performed by adding aliquots of a guest solution to the host solution or vice versa. The titrations were analyzed with a least-squares curve-fitting procedure. Control experiments involved addition of the burette solution to pure water and addition of water to the cell solution.



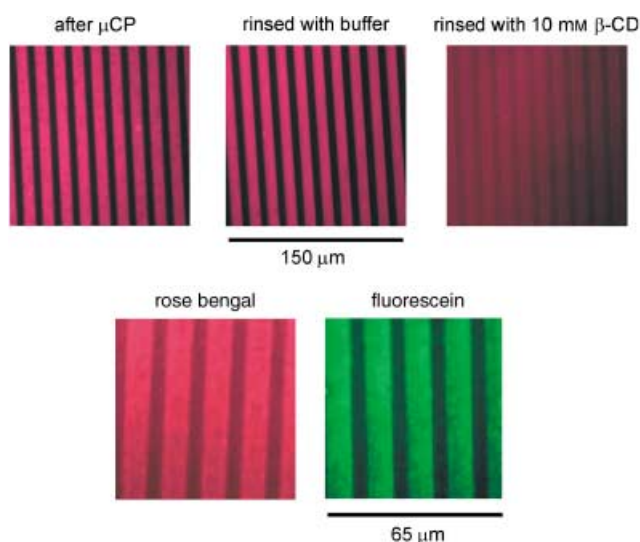


**Figure 3.** Top: confocal microscopy images after  $\mu$ CP of **3** on  $\beta$ -CD-terminated SAMs on  $\text{SiO}_2$ . Images shown are after printing, from left to right: without rinsing; after rinsing with ca. 200 mL of an aqueous buffer solution, followed by rinsing with water and drying in a stream of nitrogen; after rinsing with ca. 200 mL of 10 mM  $\beta$ -CD, followed by rinsing with water and drying in a stream of nitrogen. Dendritic wedge **3** was printed as the per- $\beta$ -CD complex from a 0.1 mM aqueous solution. The oxidized stamp was soaked in the wedge solution, blown dry with nitrogen, and brought into contact with the surface for 1 min without external pressure. Bottom: Confocal microscopy images of  $\mu$ CP of dendrimer **4a** as the per- $\beta$ -CD complex on a  $\beta$ -CD-terminated SAM on  $\text{SiO}_2$ , followed by loading with an anionic dye. The dendrimers were printed from a 0.1 mM solution in water for 1 min, without external pressure, and the patterns were washed with ca. 200 mL of 10 mM aqueous phosphate buffer (pH 7) and water to remove physisorbed material. The dendritic boxes were subsequently loaded with rose bengal (left) and fluorescein (right) by dipping the substrates in a 0.1 mM aqueous solution of the dye molecules, followed by rinsing with an aqueous buffer solution, water, and drying in a stream of nitrogen.

SPR measurements were performed in a two-channel vibrating mirror angle scan set-up based on the Kretschmann configuration, as described by Kooyman and co-workers.<sup>[28]</sup>

SIMS-TOF measurements were performed on an ION-TOF IV spectrometer (Tascon GmbH Münster, Germany) in which an  $\text{Au}_3$  gun was employed in a burst alignment mode; target current = 0.02 pA.

XPS measurements were performed on a Physical Electronics Quantum2000 equipped with a spherical sector analyzer and a multichannel plate detector (16 detector elements).

The AFM experiments were carried out with a NanoScope III multimode AFM (Digital Instruments, Santa Barbara, CA, USA) in the contact mode using V-shaped  $\text{Si}_3\text{N}_4$  cantilevers (Nanoprobes, Digital Instruments) with a spring constant of  $0.1 \text{ N m}^{-1}$ . Images were acquired in an ambient atmosphere (ca. 40–50% relative humidity,  $25^\circ\text{C}$  temperature) unless stated otherwise. A standard AFM liquid cell (Digital Instruments) was used for measurements of liquids. The sample was scanned at  $90^\circ$  with respect to the long axis of the cantilever to ensure maximum sensitivity for lateral forces in the friction force images.

Confocal microscopy images were taken on a Carl Zeiss LSM 510. The dendrimer wedge **3** and rose bengal were excited at 543 nm, while fluorescein was excited at 488 nm. The emitted fluorescence was collected on a PMT Hamamatsu R6357 spectrophotometer.

Electrochemical measurements were performed with an AUTO-LAB PGSTAT10 in a custom built three-electrode set-up equipped with a platinum counterelectrode, a mercury sulfate reference electrode ( $V_{\text{MSE}} = +0.61 V_{\text{NHE}}$ ), and a screw cap holding the gold working electrode (area exposed to the solution =  $0.44 \text{ cm}^2$ ).

Received: September 2, 2003 [Z52767]

Published Online: December 9, 2003

**Keywords:** cyclodextrins · host–guest systems · microcontact printing · nanolithography · self-assembly

- [1] J. Huskens, M. A. Deij, D. N. Reinhoudt, *Angew. Chem.* **2002**, *114*, 4647–4651; *Angew. Chem. Int. Ed.* **2002**, *41*, 4467–4471.
- [2] Y. Xia, G. M. Whitesides, *Angew. Chem.* **1998**, *110*, 568–594; *Angew. Chem. Int. Ed.* **1998**, *37*, 550–575.
- [3] B. Michel, A. Bernard, A. Bietsch, E. Delamarche, M. Geissler, D. Juncker, H. Kind, J.-P. Renault, H. Rothuizen, H. Schmid, P. Schmidt-Wenkel, R. Stutz, H. Wolf, *IBM J. Res. Dev.* **2001**, *45*, 697–719.
- [4] a) R. D. Piner, J. Zhu, F. Xu, S. Hong, C. A. Mirkin, *Science* **1999**, *283*, 661–663; b) C. A. Mirkin, S. Hong, L. Demers, *ChemPhys-Chem* **2001**, *2*, 37–39.
- [5] a) L. M. Demers, D. S. Ginger, S.-J. Park, Z. Li, S.-W. Chung, C. A. Mirkin, *Science* **2002**, *296*, 1836–1838; b) H. Zhang, Z. Li, C. A. Mirkin, *Adv. Mater.* **2002**, *14*, 1472–1474.
- [6] K.-B. Lee, S.-J. Park, C. A. Mirkin, J. C. Smith, M. Mrksich, *Science* **2002**, *295*, 1702–1705.
- [7] X. Liu, L. Fu, S. Hong, V. P. Dravid, C. A. Mirkin, *Adv. Mater.* **2002**, *14*, 231–234.
- [8] S. Hong, J. Zhu, C. A. Mirkin, *Science* **1999**, *286*, 523–525.
- [9] S. Hong, C. A. Mirkin, *Science* **2000**, *288*, 1808–1811.
- [10] M. W. J. Beulen, J. Bügler, B. Lammerink, F. A. J. Geurts, E. M. E. F. Biemond, K. G. C. van Leerdam, F. C. J. M. van Veggel, J. F. J. Engbersen, D. N. Reinhoudt, *Langmuir* **1998**, *14*, 6424–6429.
- [11] M. W. J. Beulen, J. Bügler, M. R. de Jong, B. Lammerink, J. Huskens, H. Schönherr, G. J. Vancso, B. A. Boukamp, H. Wieder, A. Offenhäuser, W. Knoll, F. C. J. M. van Veggel, D. N. Reinhoudt, *Chem. Eur. J.* **2000**, *6*, 1176–1183.
- [12] a) H. Schönherr, M. W. J. Beulen, J. Bügler, J. Huskens, F. C. J. M. van Veggel, D. N. Reinhoudt, G. J. Vancso, *J. Am. Chem. Soc.* **2000**, *122*, 4963–4967; b) S. Zapotoczny, T. Auletta, M. R. de Jong, H. Schönherr, J. Huskens, F. C. J. M. van Veggel, D. N. Reinhoudt, G. J. Vancso, *Langmuir* **2002**, *18*, 6988–6994.
- [13] M. R. de Jong, J. Huskens, D. N. Reinhoudt, *Chem. Eur. J.* **2001**, *7*, 4164–4170.
- [14] M. Mammen, S.-K. Choi, G. M. Whitesides, *Angew. Chem.* **1998**, *110*, 2908–2953; *Angew. Chem. Int. Ed.* **1998**, *37*, 2754–2794.
- [15] a) J. Rao, J. Lahiri, L. Isaacs, R. M. Weis, G. M. Whitesides, *Science* **1998**, *280*, 708–711; b) J. Rao, J. Lahiri, R. M. Weis, G. M. Whitesides, *J. Am. Chem. Soc.* **2000**, *122*, 2698–2710.
- [16] S. J. Metallo, R. S. Kane, R. E. Holmlin, G. M. Whitesides, *J. Am. Chem. Soc.* **2003**, *125*, 4534–4540.
- [17] The kinetics of  $\beta$ -CD complexes commonly follow diffusion-controlled association ( $k_i = \text{ca. } 10^9 \text{ M}^{-1} \text{ s}^{-1}$ ; J. Szejtli, *Comprehensive Supramolecular Chemistry*, Vol. 3, Pergamon, Oxford, **1996**), and thus dissociation rates follow directly from association rates and thermodynamics.
- [18] Microcalorimetry gave an intrinsic binding constant for the Ad- $\beta$ -CD interaction of  $5.0 \times 10^4 \text{ M}^{-1}$  and a binding enthalpy of  $-7.5 \text{ kcal mol}^{-1}$  for calixarene guest **2**.
- [19] J. J. Michels, J. Huskens, D. N. Reinhoudt, *J. Am. Chem. Soc.* **2002**, *124*, 2056–2064.
- [20] The stoichiometry (1:1), the  $K$  value ( $1.4 \times 10^7 \text{ M}^{-1}$ ), and the binding enthalpy ( $-16.2 \text{ kcal mol}^{-1}$ ) indicate that both Ad

groups of the guest interact with both  $\beta$ -CD cavities of the dimer to form a 1:1 complex.

- [21] Value obtained for a 1:1 model in which the  $\beta$ -CD SAM is treated as a SAM of dimeric hosts with a concentration of half the  $\beta$ -CD concentration at the surface.
- [22] The contrast in the AFM images does not allow any conclusion on the amount of ink present on the patterns directly after printing or after subsequent washing. XPS and EIS measurements showed that: a) three to five monolayers of guest ink are transferred by  $\mu$ CP onto both OH- and  $\beta$ -CD-terminated SAMs; b) approximately one monolayer of guests is present after a first rinsing of the  $\beta$ -CD-terminated SAMs with water; c) submonolayer coverages remain on the  $\beta$ -CD-terminated SAMs upon prolonged washing with water and  $\beta$ -CD solutions (See Supporting Information). A monolayer is defined as a layer of the calixarene guest molecules bound through both Ad groups to two  $\beta$ -CD cavities at the surface.
- [23] In contrast, patterns created on a reference polyethyleneglycol monolayer (A. Papra, N. Gadegaard, N. B. Larsen, *Langmuir* **2001**, *17*, 1457–1460) were removed easily by rinsing with an aqueous buffer solution.
- [24] J. J. Michels, M. W. P. L. Baars, E. W. Meijer, J. Huskens, D. N. Reinhoudt, *J. Chem. Soc. Perkin Trans. 2* **2000**, 1914–1918.
- [25] a) J. F. G. A. Jansen, E. M. M. de Brabander-van den Berg, E. W. Meijer, *Science* **1994**, *266*, 1226–1229b) J. F. G. A. Jansen, H. W. I. Peerlings, E. M. M. de Brabander-van den Berg, E. W. Meijer, *Angew. Chem.* **1995**, *107*, 1321–1324; *Angew. Chem. Int. Ed. Engl.* **1995**, *34*, 1206–1209.
- [26] R. Castro, I. Cuadro, B. Alonso, C. M. Casado, M. Morán, A. E. Kaifer, *J. Am. Chem. Soc.* **1997**, *119*, 5760–5761.
- [27] I. Cuadro, M. Morán, C. M. Casado, B. Alonso, F. Lobete, B. Carciá, M. Ibisate, J. Losada, *Organometallics* **1996**, *15*, 5278–5280.
- [28] A. T. M. Lenferink, R. P. H. Kooyman, J. Greve, *Sens. Actuators B* **1991**, *3*, 261–265.